Clinical targeting of HIV capsid protein with a long-acting small molecule

https://doi.org/10.1038/s41586-020-2443-1

Received: 26 November 2019

Accepted: 14 April 2020

Published online: 1 July 2020

Check for updates

A list of authors and their affiliations appears at the end of the paper.

Oral antiretroviral agents provide life-saving treatments for millions of people living with HIV, and can prevent new infections via pre-exposure prophylaxis[1–5]. However, some people living with HIV who are heavily treatment-experienced have limited or no treatment options, owing to multidrug resistance[6]. In addition, suboptimal adherence to oral daily regimens can negatively affect the outcome of treatment—which contributes to virologic failure, resistance generation and viral transmission—as well as of pre-exposure prophylaxis, leading to new infections[1,2,4,7–9]. Long-acting agents from new antiretroviral classes can provide much-needed treatment options for people living with HIV who are heavily treatment-experienced, and additionally can improve adherence[10]. Here we describe GS-6207, a small molecule that disrupts the functions of HIV capsid protein and is amenable to long-acting therapy owing to its high potency, low in vivo systemic clearance and slow release kinetics from the subcutaneous injection site. Drawing on X-ray crystallographic information, we designed GS-6207 to bind tightly at a conserved interface between capsid protein monomers, where it interferes with capsid-protein-mediated interactions between proteins that are essential for multiple phases of the viral replication cycle. GS-6207 exhibits antiviral activity at picomolar concentrations against all subtypes of HIV-1 that we tested, and shows high synergy and no cross-resistance with approved antiretroviral drugs. In phase-1 clinical studies, monotherapy with a single subcutaneous dose of GS-6207 (450 mg) resulted in a mean $\log_{10}$-transformed reduction of plasma viral load of 2.2 after 9 days, and showed sustained plasma exposure at antivirally active concentrations for more than 6 months. These results provide clinical validation for therapies that target the functions of HIV capsid protein, and demonstrate the potential of GS-6207 as a long-acting agent to treat or prevent infection with HIV.

HIV-1 capsid protein (p24; hereafter abbreviated CA) has essential roles throughout the viral replication cycle, making it an attractive target for therapeutic intervention[11,12]. Unlike the viral enzymes (protease, reverse transcriptase and integrase) that are currently targeted by small-molecule antiretroviral drugs, CA functions through interactions between proteins; targets that function in this way have historically posed considerable challenges for interventions using small-molecule drugs[13]. CA is initially expressed within the Gag and Gag–Pol polyproteins, and provides key interactions between proteins that are necessary for assembly of the virion[14]. In the virion, CA is released by precursor cleavage mediated by HIV-1 protease, and self-assembles into a conical capsid composed of about 250 CA hexamers and 12 pentamers[15]. The correct formation and integrity of the capsid are essential for virus infectivity[14]. Upon infection of a new cell, controlled intracellular transport and disassembly of the viral capsid is regulated, in part, by interactions with host factors, and supports reverse transcription and proviral DNA integration[16–18].

We assayed small molecules for effects on the kinetics of in vitro CA assembly, and identified multiple inhibitor and accelerator series. Potency improvements through chemical modification were limited for compounds that inhibited CA assembly, presumably because these compounds could not overcome mass action and excess of the CA subunit in the virion (about 4 mM)[19,20]. Compounds that worked in concert with mass action to increase the rate and extent of CA assembly proved more amenable to improvement of their antiviral activity. Ultimately, extensive potency and pharmacokinetic optimization was required to discover a clinical candidate directed against HIV CA. The activity of GS-CA1 has previously been reported[21]. Here we report on GS-6207 (Fig. 1a), a CA-targeting inhibitor of HIV replication that is even more potent and more metabolically stable than GS-CA1 and that is suitable for clinical trials[22]. GS-6207 showed a dose-dependent increase in the rate and extent of in vitro CA assembly (Fig. 1b). In a cellular context, this acceleration of CA assembly produced malformed capsids that are morphologically distinct from mature and immature particles (Fig. 1c, d). Importantly, GS-6207 showed a mean half-maximum effective concentration (EC_{50}) of 105 pM in MT-4 cells infected with HIV-1, which makes this inhibitor significantly more potent than all of the approved HIV antiretroviral drugs that we tested (Fig. 1e). GS-6207 showed picomolar mean EC_{50} values in primary human $CD4^+$ T cells (32 pM) and macrophages (56 pM) infected with HIV-1, and remained broadly active against 2 HIV-2 isolates (885 pM) and 23 clinical HIV-1 isolates (50 pM, range of 20 to 160 pM) in human peripheral blood mononuclear cells (Fig. 1f). GS-6207 exhibited minimal cytotoxicity in human cell lines and primary cells, showing a mean half-maximal

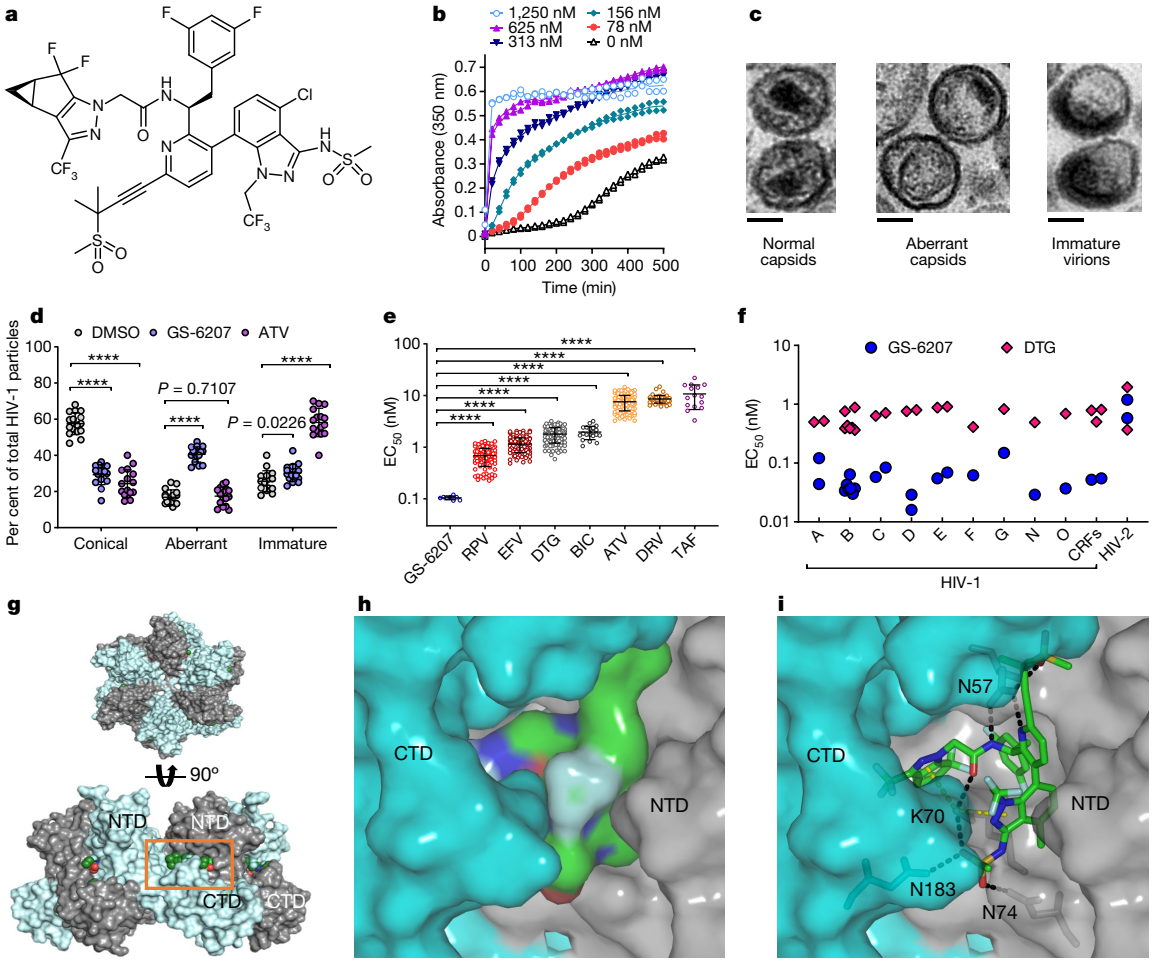

Fig. 1 | GS-6207 is a potent CA-targeting inhibitor of HIV replication. a, GS-6207. **b**, Light scattering (absorbance at 350 nm) responses showing the rate and extent of in vitro CA (20 μM) assembly in 2 M NaCl, in the presence and absence of GS-6207. Data are representative of four independent experiments ($n = 2$ biological replicates each). **c**, Representative thin-section electron micrograph images of HIV-1 produced in the presence of 0.2% dimethyl sulfoxide (DMSO) (left), GS-6207 (15 nM) (middle) or the HIV-1 protease inhibitor atazanavir (500 nM) (right). Scale bars, 50 nm. **d**, Quantification for **c**. Data are mean ± s.d. from representative images of HIV-1 produced in one of two independent experiments. DMSO, $n = 737$ virions; GS-6207, $n = 591$ virions; atazanavir (ATV), $n = 618$ virions. *P* values in all figures are by unpaired two-tailed Student's *t*-test with Welch's correction. $^{****}P < 0.0001$. **e**, Inhibition of HIV-1 strain IIIB in MT-4 cells. Data are mean ± s.d. from 4 biological replicates in each of 8 to 115 independent experiments. GS-6207 ($n = 8$), rilpivirine (RPV) ($n = 113$), efavirenz (EFV) ($n = 113$), dolutegravir (DTG) ($n = 115$), bictegravir (BIC) ($n = 20$), ATV ($n = 113$), darunavir (DRV) ($n = 60$) and tenofovir alafenamide (TAF) ($n = 15$). $^{****}P < 1 \times 10^{-15}$. **f**, Inhibition of HIV-2 and HIV-1 group M (subtypes A–G, circulating recombinant forms (CRFs)), N and O clinical isolates. Data represent individual isolates ($n = 3$ biological replicates each). **g**, X-ray crystal structure of GS-6207–CA hexamer complex. Top and side views of CA hexamer (individual CA monomers coloured alternately in cyan and grey). The GS-6207 binding site, located between the NTD of one CA monomer and the CTD of an adjacent monomer, is boxed. **h**, Space-filling view of GS-6207 in its binding site (X-ray structure). **i**, Hydrogen bonds (dashed black lines, $n = 7$) and cation–π interactions (dashed yellow lines, $n = 2$) are shown between GS-6207 and CA residues.

cytotoxic concentration (CC_{50}) in peripheral blood mononuclear cells of >50 μM and a therapeutic index (CC_{50}/EC_{50}) of more than 1,000,000 (Extended Data Table 1). When combined with other antiretroviral agents, GS-6207 displayed synergy (Extended Data Table 2) and retained full activity against HIV-1 variants that are resistant to current drug classes (Extended Data Table 3), which demonstrates its potency in combination and against drug-resistant strains of HIV.

The molecular underpinnings of the role of GS-6207 as an accelerator of CA monomer assembly are apparent in a 2.0 Å resolution X-ray crystal structure of GS-6207 in complex with a cross-linked CA hexamer (Fig. 1g–i, Extended Data Table 4). In this structure, GS-6207 binding is located between the N-terminal domain of one subunit of the CA hexamer (CA_{NTD}) and the C-terminal domain (CA_{CTD}) of an adjacent subunit in the hexamer. GS-6207 exhibits notable shape complementarity with adjacent CA monomers (contacting more than 2,000 $Å^2$ of buried protein surface area), and displays extensive hydrophobic and electrostatic interactions that include two cation–π interactions and seven hydrogen bonds. The GS-6207 sulfonamide is the linchpin in a hydrogen-bonding network that bridges from CA_{NTD} residues N74 and K70 of one subunit to CA_{CTD} residue N183 of the neighbouring subunit, and orders a loop that is unstructured in the apo hexamer crystal (Fig. 1i). Consistent with its binding position between neighbouring CA monomers in this crystal structure, GS-6207 showed saturable dose-dependent binding to Gag and CA; the slow dissociation of GS-6207 from CA multimers is consistent with a tenfold-higher affinity relative to the CA monomer (Extended Data Table 5).

To define the functional consequences of GS-6207 binding to capsid, we measured the potency of GS-6207 during early and late stages of the viral replication cycle in target MT-2 and producer HEK293T cells, respectively. GS-6207 showed sub-nanomolar potency in target cells ($EC_{50} = 23$ pM), in a full-cycle assay ($EC_{50} = 25$ pM) and in producer cells ($EC_{50} = 439$ pM), which indicates that GS-6207 interferes with both the early and late stages of HIV-1 replication but exhibits greater potency against the early stage (Fig. 2a). Time-of-addition

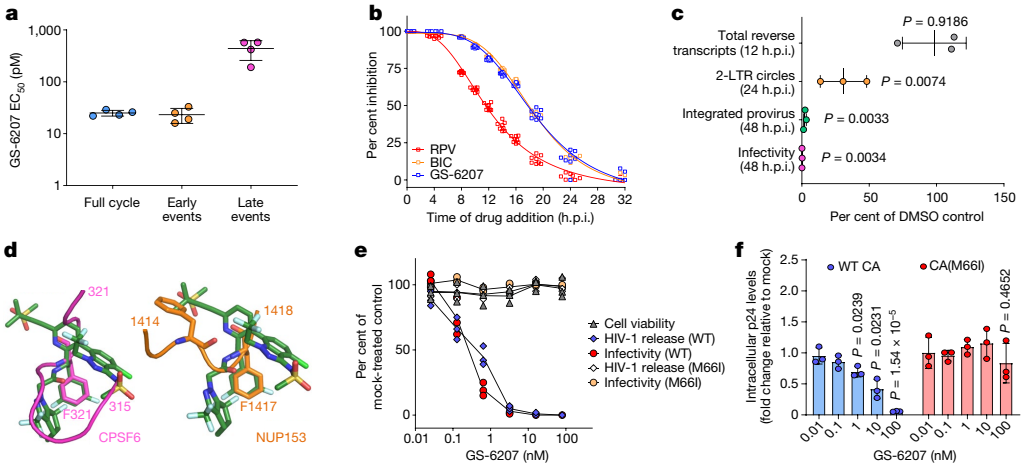

Fig. 2 | GS-6207 inhibits multiple CA-dependent steps of HIV-1 replication. **a**, Antiviral activity of GS-6207 throughout a full replication cycle, or when selectively present during target-cell infection (early events) or virus production (late events). Data are mean ± s.d. from 4 independent experiments ($n = 3$ biological replicates each). **b**, Time-of-addition study indicating when GS-6207 inhibits HIV-1 replication relative to rilpivirine (reverse transcriptase inhibitor) and bictegravir (integrase inhibitor). Data are mean from one of two representative independent experiments ($n = 8$ biological replicates per group in each experiment). h.p.i., hours post-infection. **c**, Effect of GS-6207 (1.25 nM) on the intracellular abundance of various forms of HIV-1 DNA. Data are mean ± s.d. from one of two representative independent experiments ($n = 3$ biological replicates each). **d**, Overlay of GS-6207 with CA-binding peptides from nuclear-import factors CPSF6 and NUP153 (ref. [25]) in their shared binding pocket. **e**, Effect of GS-6207 on HEK293T producer-cell viability, HIV-1 particle production and infectivity. Data are mean from one of three representative independent experiments ($n = 3$ biological replicates each). M66I, GS-6207 resistance-associated CA-binding-site variant; WT, wild type. **f**, Effect of GS-6207 on intracellular p24 levels. Data are mean ± s.d. from 3 independent experiments ($n = 3$ biological replicates each). For gel source data, see Supplementary Fig. 1.

studies relative to a non-nucleoside reverse-transcriptase inhibitor and an integrase strand-transfer inhibitor indicated that GS-6207 targets one or more steps that occur after reverse transcription and before integration (Fig. 2b). In quantitative PCR assays, we measured the accumulation of the products of reverse transcription, the formation of two-long-terminal-repeat (2-LTR) circles (which indicate nuclear localization but aborted integration) and proviral integration (Fig. 2c). GS-6207 at 1.25 nM (12.5-fold EC_{50}) did not alter the synthesis of HIV complementary DNA (cDNA) but significantly reduced formation of 2-LTR circles and integrated proviruses. These data suggest that GS-6207 might prevent the nuclear import of viral cDNA—possibly via direct competition with host-cell nuclear import cofactors (such as nucleoporin 153 (NUP153) and cleavage and polyadenylation specificity factor 6 (CPSF6)[23–26]) that bind CA and share a CA binding site with GS-6207 (Fig. 2d). In addition to these early effects and the effects on capsid formation, GS-6207 inhibited the production of HIV-1 that contains mature wild-type CA but not the CA(M66I) binding-site mutant that reduces GS-6207 binding affinity to CA oligomers (Extended Data Table 5), as measured by a p24 enzyme-linked immunosorbent assay (Fig. 2e). GS-6207 did not inhibit HIV-1 protease cleavage activity in vitro (half-maximal inhibitory concentration of more than 50 μM) but reduced intracellular Gag and processed CA levels in the producer cells (Fig. 2f), which indicates that the loss of p24 production probably reflected GS-6207 binding to CA precursors, and a reduction in Gag and/or Gag–Pol stability, trafficking and/or viral assembly.

To evaluate drug resistance, we serially passaged HIV-1 in MT-2 cells in the presence of increasing concentrations of GS-6207 for more than three months (Fig. 3a). Sequence analysis identified an N74D substitution in CA (passages 4–6) followed by a CA(Q67H/N74D) variant (passages 7–10). The N74D substitution has previously been shown to alter the viral pathway of nuclear entry[27]. Viruses with these GS-6207 resistance-associated mutations remained fully sensitive to agents from other antiretroviral classes (Fig. 3b). Selections performed in the presence of fixed concentrations of GS-6207 in human peripheral blood mononuclear cells independently infected with six HIV-1 isolates similarly identified Q67H and N74D as the major resistance-associated

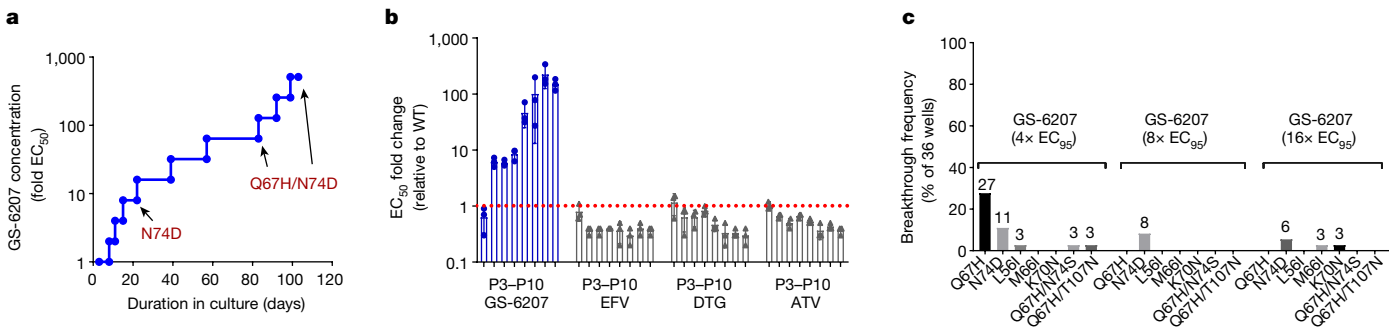

Fig. 3 | Resistance to GS-6207 maps to CA. **a**, Emergent CA substitutions denoted during resistance selection in MT-2 cells infected with HIV-1 strain HXB2D, by escalation of the GS-6207 dose. Data are representative of one of two biological replicates from a single selection experiment. **b**, Fold resistance of GS-6207-selected viral isolate passage (P)3 to 10 (each tick mark corresponds to one passage) to GS-6207, and control antiretroviral agents. Data are mean ± s.d. from 3 independent experiments ($n = 3$ biological replicates each). Red dotted line defines the cut-off for drug resistance. **c**, Frequency of GS-6207-selected CA variants observed at fixed GS-6207 concentrations in peripheral blood mononuclear cells infected with clinical HIV-1 isolates.

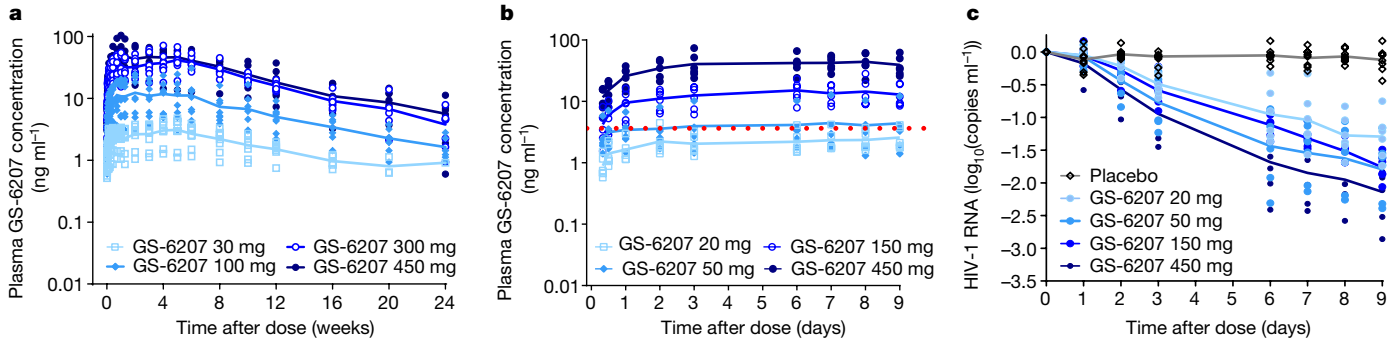

Fig. 4 | Clinical testing of GS-6207 in humans. a, Mean plasma concentration–time profile of GS-6207 after a single subcutaneous administration of 30–450 mg of drug to uninfected individuals ($n = 8$ within each dosing arm). **b**, Mean plasma concentration–time profile of GS-6207 after a single subcutaneous administration of 20–450 mg to individuals infected with HIV ($n = 6$ within each dosing arm). Red dotted line defines protein-adjusted EC_{95} for GS-6207. **c**, Mean log_{10}-transformed change in plasma HIV-1 RNA after a single subcutaneous administration of 20–450 mg GS-6207 to 8 individuals with untreated HIV-1 infection randomized to drug ($n = 6$) or placebo ($n = 2$) within each dosing arm.

mutations, with additional variants (L56I, M66I, K70N, Q67H/N74S and Q67H/T107N) that were each independently detected in a single GS-6207-selected culture (Fig. 3c). These resistance-associated mutations, alone or in combination, conferred reduced susceptibility to GS-6207 (6- to >3,200-fold resistance relative to the wild-type virus), consistent with the assignment of CA as the functional target of GS-6207. All CA residues that confer resistance map to the GS-6207 binding site and are highly conserved across subtypes of HIV-1[21,28–30]. Of the mutants that we tested, all but the low-level-resistant Q67H variant (sixfold resistance to GS-6207 relative to wild-type virus) display reduced replication capacity in vitro (Extended Data Table 6).

Low hepatic clearance is an essential attribute for a long-acting agent. Thus, along with enhancement of potency, the design process that culminated in GS-6207 also focused on blocking metabolically labile sites through incorporation of electron-withdrawing groups (halogens and sulfonyls), metabolically stable ring systems (cyclopropane and pyrazoles) and rigidifying elements. Tritiation ([^{3}H]) of GS-6207 was necessary to accurately measure the low turnover of GS-6207 in primary human hepatocytes, and showed a predicted rate of hepatic clearance of 0.011 $l\ h^{-1}\ kg^{-1}$, or 0.8% of the hepatic extraction.

In a single-ascending-dose clinical study that was randomized, double-blind and placebo-controlled, we administered a suspension formulation of 30 to 450 mg GS-6207 to healthy participants (32 active and 8 placebo)—most of whom were male (27 of 40) and in their 30s (median age of 37 years old, range 19 to 44 years old), and had normal kidney and liver function—as a subcutaneous injection (Fig. 4a). Consistent with nonclinical safety studies, GS-6207 was generally safe and well-tolerated. The most frequent adverse events were mild erythema and/or pain at the injection site that resolved in a few days (Extended Data Table 7). GS-6207 pharmacokinetic profiles showed slow, sustained drug release, with a median apparent terminal half-life ($t_{1/2}$) of about 38 days. Increases in exposure to GS-6207 were approximately dose-proportional. At doses of ≥100 mg, GS-6207 plasma concentrations exceeded the human serum protein-adjusted 95% effective concentration (EC_{95}) for wild-type HIV-1 (4.0 nM or 3.87 ng ml^{-1} in MT-4 cells) for ≥12 weeks, and doses of ≥300 mg exceeded the human protein-adjusted EC_{95} for more than 24 weeks.

In a subsequent clinical study (which was also randomized, double-blind and placebo-controlled), 20 to 450 mg GS-6207 was administered to trial participants with untreated HIV-1 infection (24 active and 8 placebo) as a single-dose subcutaneous suspension. We conducted a prespecified interim analysis of this part of the study. Most of the participants were male (30 of 32), in their 30s (median age of 34 years old, range 19 to 59 years old) and treatment-naive (25 of 32), and had median HIV-1 RNA loads of log_{10}-transformed copies per millilitre of 4.48 (range of 3.86 to 5.01) and median $CD4^+$ T cell counts of 458 cells per microlitre (range of 200 to 1,009). GS-6207 was generally safe and well-tolerated (Extended Data Table 8), and the concentration–time profiles of GS-6207 were consistent with those in HIV-negative participants through to nine days after administration of the dose (Fig. 4b, Extended Data Table 9). A single subcutaneous administration of 20, 50, 150 or 450 mg GS-6207 led to mean maximum log_{10}-transformed reductions of 1.35, 1.79, 1.76 and 2.20, respectively, in plasma HIV-1 RNA by the ninth day (Fig. 4c, Extended Data Table 10). A genetic mixture of wild-type CA and the CA(Q67H) mutant emerged on day 9 in one participant in the 20-mg cohort, which was associated with a 1.6-fold decrease in phenotypic susceptibility but not with viral escape by day 9 of monotherapy.

These data establish GS-6207 as a first-in-class HIV-1 capsid inhibitor with potent antiviral activity against both wild-type virus and variants that are resistant to current antiretroviral agents. The favourable safety profile, prolonged pharmacokinetic exposure and observed antiviral efficacy in humans support continued clinical development of GS-6207 as a long-acting antiretroviral agent for the treatment of infection with HIV-1, including for people living with HIV who are heavily treatment-experienced and have multidrug-resistant virus. In addition, the infrequent subcutaneous dosing renders GS-6207 an attractive candidate for the simplified prevention of the acquisition of HIV in at-risk populations—making this drug a potentially transformative tool in efforts to end the global HIV epidemic.

Online content

Any methods, additional references, Nature Research reporting summaries, source data, extended data, supplementary information, acknowledgements, peer review information; details of author contributions and competing interests; and statements of data and code availability are available at https://doi.org/10.1038/s41586-020-2443-1.

1. Grant, R. M. et al. Preexposure chemoprophylaxis for HIV prevention in men who have sex with men. *N. Engl. J. Med.* **363**, 2587–2599 (2010).
2. Baeten, J. M. et al. Antiretroviral prophylaxis for HIV prevention in heterosexual men and women. *N. Engl. J. Med.* **367**, 399–410 (2012).
3. Molina, J. M. et al. On-demand preexposure prophylaxis in men at high risk for HIV-1 infection. *N. Engl. J. Med.* **373**, 2237–2246 (2015).
4. Thigpen, M. C. et al. Antiretroviral preexposure prophylaxis for heterosexual HIV transmission in Botswana. *N. Engl. J. Med.* **367**, 423–434 (2012).
5. WHO. HIV/AIDS Fact Sheets, 15 November 2019. https://www.who.int/news-room/fact-sheets/detail/hiv-aids (WHO, 2019).
6. Emu, B. et al. Phase 3 study of ibalizumab for multidrug-resistant HIV-1. *N. Engl. J. Med.* **379**, 645–654 (2018).
7. Bangsberg, D. R. et al. Non-adherence to highly active antiretroviral therapy predicts progression to AIDS. *AIDS* **15**, 1181–1183 (2001).
8. Marrazzo, J. M. et al. Tenofovir-based preexposure prophylaxis for HIV infection among African women. *N. Engl. J. Med.* **372**, 509–518 (2015).
9. Anderson, P. L. et al. Emtricitabine–tenofovir concentrations and pre-exposure prophylaxis efficacy in men who have sex with men. *Sci. Transl. Med.* **4**, 151ra125 (2012).

10. Gulick, R. M. & Flexner, C. Long-acting HIV drugs for treatment and prevention. *Annu. Rev. Med.* **70**, 137–150 (2019).
11. Thenin-Houssier, S. & Valente, S. T. HIV-1 capsid inhibitors as antiretroviral agents. *Curr. HIV Res.* **14**, 270–282 (2016).
12. Carnes, S. K., Sheehan, J. H. & Aiken, C. Inhibitors of the HIV-1 capsid, a target of opportunity. *Curr. Opin. HIV AIDS* **13**, 359–365 (2018).
13. Scott, D. E., Bayly, A. R., Abell, C. & Skidmore, J. Small molecules, big targets: drug discovery faces the protein–protein interaction challenge. *Nat. Rev. Drug Discov.* **15**, 533–550 (2016).
14. Freed, E. O. HIV-1 assembly, release and maturation. *Nat. Rev. Microbiol.* **13**, 484–496 (2015).
15. Ganser, B. K., Li, S., Klishko, V. Y., Finch, J. T. & Sundquist, W. I. Assembly and analysis of conical models for the HIV-1 core. *Science* **283**, 80–83 (1999).
16. Yamashita, M. & Engelman, A. N. Capsid-dependent host factors in HIV-1 infection. *Trends Microbiol.* **25**, 741–755 (2017).
17. Huang, P. T. et al. FEZ1 is recruited to a conserved cofactor site on capsid to promote HIV-1 trafficking. *Cell Rep.* **28**, 2373–2385 (2019).
18. Fernandez, J. et al. Transportin-1 binds to the HIV-1 capsid via a nuclear localization signal and triggers uncoating. *Nat. Microbiol.* **4**, 1840–1850 (2019).
19. Carlson, L. A. et al. Three-dimensional analysis of budding sites and released virus suggests a revised model for HIV-1 morphogenesis. *Cell Host Microbe* **4**, 592–599 (2008).
20. Briggs, J. A., Wilk, T., Welker, R., Kräusslich, H. G. & Fuller, S. D. Structural organization of authentic, mature HIV-1 virions and cores. *EMBO J.* **22**, 1707–1715 (2003).
21. Yant, S. R. et al. A highly potent long-acting small-molecule HIV-1 capsid inhibitor with efficacy in a humanized mouse model. *Nat. Med.* **25**, 1377–1384 (2019).
22. Graupe, M. et al. Therapeutic compounds. US patent 10,071,985 B2 (2018).
23. Matreyek, K. A., Yücel, S. S., Li, X. & Engelman, A. Nucleoporin NUP153 phenylalanine-glycine motifs engage a common binding pocket within the HIV-1 capsid protein to mediate lentiviral infectivity. *PLoS Pathog.* **9**, e1003693 (2013).
24. Price, A. J. et al. CPSF6 defines a conserved capsid interface that modulates HIV-1 replication. *PLoS Pathog.* **8**, e1002896 (2012).
25. Price, A. J. et al. Host cofactors and pharmacologic ligands share an essential interface in HIV-1 capsid that is lost upon disassembly. *PLoS Pathog.* **10**, e1004459 (2014).
26. Bhattacharya, A. et al. Structural basis of HIV-1 capsid recognition by PF74 and CPSF6. *Proc. Natl Acad. Sci. USA* **111**, 18625–18630 (2014).
27. Lee, K. et al. Flexible use of nuclear import pathways by HIV-1. *Cell Host Microbe* **7**, 221–233 (2010).
28. Perrier, M. et al. Prevalence of gag mutations associated with in vitro resistance to capsid inhibitor GS-CA1 in HIV-1 antiretroviral-naive patients. *J. Antimicrob. Chemother.* **72**, 2954–2955 (2017).
29. Li, G. et al. Functional conservation of HIV-1 Gag: implications for rational drug design. *Retrovirology* **10**, 126 (2013).
30. Yant, S. R. et al. In vitro resistance profile of GS-6207, a first-in-class picomolar HIV capsid inhibitor in clinical development as a novel long-acting antiretroviral agent. In *10th IAS Conference on HIV Science* http://programme.ias2019.org/Abstract/Abstract/683 (IAS, 2019).

John O. Link[1], Martin S. Rhee[1], Winston C. Tse[1,8], Jim Zheng[1], John R. Somoza[1], William Rowe[1], Rebecca Begley[1], Anna Chiu[1], Andrew Mulato[1], Derek Hansen[1], Eric Singer[1], Luong K. Tsai[1], Rujuta A. Bam[1], Chien-Hung Chou[1], Eda Canales[1], Gediminas Brizgys[1], Jennifer R. Zhang[1], Jiayao Li[1], Michael Graupe[1], Philip Morganelli[1], Qi Liu[1,9], Qiaoyin Wu[1], Randall L. Halcomb[1,10], Roland D. Saito[1,8], Scott D. Schroeder[1], Scott E. Lazerwith[1], Steven Bondy[1], Debi Jin[1], Magdeleine Hung[1], Nikolai Novikov[1], Xiaohong Liu[1], Armando G. Villaseñor[1], Carina E. Cannizzaro[1], Eric Y. Hu[1], Robert L. Anderson[1,11], Todd C. Appleby[1], Bing Lu[1], Judy Mwangi[1], Albert Liclican[1], Anita Niedziela-Majka[1], Giuseppe A. Papalia[1], Melanie H. Wong[1], Stephanie A. Leavitt[1], Yili Xu[1], David Koditek[1], George J. Stepan[1], Helen Yu[1], Nikos Pagratis[1], Sheila Clancy[1], Shekeba Ahmadyar[1], Terrence Z. Cai[1,12], Scott Sellers[1], Scott A. Wolckenhauer[1], John Ling[1], Christian Callebaut[1], Nicolas Margot[1], Renee R. Ram[1], Ya-Pei Liu[1], Rob Hyland[1], Gary I. Sinclair[2], Peter J. Ruane[3], Gordon E. Crofoot[4], Cheryl K. McDonald[5], Diana M. Brainard[1], Latesh Lad[1], Swami Swaminathan[1], Wesley I. Sundquist[6], Roman Sakowicz[1], Anne E. Chester[1], William E. Lee[1], Eric S. Daar[7], Stephen R. Yant[1]✉ & Tomas Cihlar[1]

[1]Gilead Sciences, Foster City, CA, USA. [2]AIDS Arms Inc, DBA Prism Health North Texas, Dallas, TX, USA. [3]Ruane Clinical Research Group Inc, Los Angeles, CA, USA. [4]The Crofoot Research Center Inc, Houston, TX, USA. [5]Texas Centers for Infectious Disease Associates, Fort Worth, TX, USA. [6]Department of Biochemistry, University of Utah School of Medicine, Salt Lake City, UT, USA. [7]Division of HIV Medicine at Harbor-UCLA Medical Center, David Geffen School of Medicine at UCLA, Torrance, CA, USA. [8]Present address: Vir Biotechnology Inc, San Francisco, CA, USA. [9]Present address: Center for Drug Evaluation and Research, US Food and Drug Administration, Silver Spring, MD, USA. [10]Present address: Terns Pharmaceuticals, Foster City, CA, USA. [11]Present address: MyoKardia Inc, South San Francisco, CA, USA. [12]Present address: Bayer, Berkeley, CA, USA. ✉e-mail: stephen.yant@gilead.com

Methods

No statistical methods were used to predetermine sample size. The in vitro experiments were not randomized and investigators were not blinded to sample allocation during in vitro experiments and outcome assessment.

Compounds

GS-6207 was synthesized at Gilead Sciences, and chemical identity (^{1}H-nuclear magnetic resonance (NMR), ^{13}C-NMR and high-resolution mass-spectrometry spectra) and sample purity were established using reverse-phase high-performance liquid chromatography (HPLC) (Supplementary Information). The control antiretroviral agents emtricitabine (FTC), tenofovir alafenamide (TAF), elvitegravir (EVG), raltegravir (RAL), bictegravir (BIC), darunavir (DRV), atazanavir (ATV) and bevirimat (BVM) were synthesized at Gilead Sciences, and efavirenz (EFV) and dolutegravir (DTG) were purchased from Toronto Research Chemicals and Porton Shanghai R&D Center, respectively. Puromycin (a control compound for cytotoxicity assays) was purchased from Sigma-Aldrich.

Viruses

The HIV-1 strains IIIB and BaL were obtained from the NIH AIDS Reagent Program and from Advanced Biotechnologies, respectively. Two HIV-2 isolates (CBL20 and CDC310319) and 23 clinical HIV-1 isolates from the Southern Research virus collection were selected for susceptibility profiling: subtype A (92UG031 and 92UG037), subtype B (89BZ_167, 90US_873, YU-2, 91US001, 91US004, 96TH_NP1538, BaL and JR-CSF), subtype C (92BR025 and 98US_MSC5016), subtype D (92UG001 and 98UG_57128), subtype E (CMU02 and CMU08), subtype F (93BR020), subtype G (JV1083), group N (YBF30), group O (BCF01), CRF01_AE (90TH_CM235) and CRF02_AG (01CM0008BBY, 91DJ263). HIV-1 recombinant strains encoding mutation(s) that confer resistance to nucleoside reverse transcriptase inhibitors, non-nucleoside reverse transcriptase inhibitors, integrase strand transfer inhibitors, protease inhibitors or maturation inhibitors have previously been described[31,32]. Single-cycle HIV-1 encoding firefly luciferase with and without mutations within the capsid gene was made by co-transfecting HEK293T cells with pKS13ΔEnv and pHCMV-G plasmids. Cell-free viral supernatant was collected 3 days after transfection, clarified using a 0.45-μm syringe filter and stored at −80 °C. The amount of HIV in each sample was quantified by p24 antigen enzyme-linked immunosorbent assay (Perkin Elmer) and a reverse transcriptase activity assay (Southern Research).

Cell lines

Human MT-2 and MT-4 T-cell lines were obtained from the NIH AIDS Reagent Program and maintained in RPMI-1640 medium supplemented with 10% heat-inactivated fetal bovine serum (FBS), 100 units ml^{-1} penicillin, and 10 μg ml^{-1} streptomycin (complete RPMI). MT-2 cells chronically infected with HIV-1 strain IIIB were cultured in complete RPMI. HEK293T cells were obtained from the Gladstone Institute for Virology and Immunology and maintained in Dulbecco's modified Eagle's medium (DMEM) supplemented with 10% FBS, 100 units ml^{-1} penicillin, and 10 μg ml^{-1} streptomycin (complete DMEM). The human hepatoma Huh-7 cell line was obtained from ReBLikon and cultured in complete DMEM[33]. The human hepatoblastoma cell line HepG2, human prostate carcinoma cell line PC-3 and normal human fetal-lung-derived MRC-5 cells were obtained from the American Type Culture Collection. PC-3 and HepG2 cells were adapted to grow in 0.2% galactose-containing, glucose-free DMEM supplemented with 10% FBS, 1% non-essential amino acids, 1% pyruvate, and 1% GlutaMAX. MRC-5 cells were maintained in Eagle's Minimum Essential Medium (MEM) supplemented with 10% FBS. Each cell culture medium was further supplemented with 100 units ml^{-1} penicillin and 100 μg ml^{-1} streptomycin. The above eukaryotic cell lines were not authenticated and were judged to be free of mycoplasma contamination using the MycoProbe Mycoplasma Detection Kit (R&D Systems).

Primary cells

Human peripheral blood mononuclear cells (PBMCs) were collected from healthy volunteers under informed consent; their use was approved by an institutional review board at AllCells. The preparation of human PBMCs, CD4$^+$ T lymphocytes and monocyte-derived macrophage cultures have previously been described[31]. Before infection, PBMCs and CD4$^+$ T cells were activated for 48 h at 37 °C by addition of 1 μg ml^{-1} phytohaemagglutinin (PHA) and 50 international units ml^{-1} recombinant human interleukin 2 (IL-2). Primary human hepatocytes from three independent donors were purchased from Invitrogen and cultured in William's Medium E medium containing cell maintenance supplement. Donor profiles were limited to 4–65 years of age, non-smokers with limited alcohol consumption. Upon arrival at Gilead Sciences, hepatocytes were allowed to recover in a 37-°C incubator with 5% CO_2 and 90% humidity for 12–18 h in complete medium with vendor-supplied supplements before treatment with compounds.

Antiviral assays

The five-day cytoprotection antiviral assays using MT-2 and MT-4 T-cell lines have previously been described[31]. Data analysis was performed using GraphPad Prism 7.0 to calculate EC_{50} values. The EC_{95} value for GS-6207 was calculated from the EC_{50} and Hill coefficient, n, determined in MT-4 cells using the equation: $EC_{95} = EC_{50} \times (95/5)^{1/n}$.

For time-of-addition antiviral assays, MT-2 cells were infected with single-cycle reporter HIV-1 for 1 h at 37 °C, washed and seeded into 96-well plates (75-μl aliquots; 1.5×10^4 cells per well). A 25-μl aliquot of complete RPMI medium was added to 8 uninfected and 8 infected wells as respective minimum (0%) and maximal (100%) infection controls. Twenty-five-microlitre aliquots of 4× drug–medium were added to 8 replicate wells at indicated times after infection. GS-6207 and control antiretroviral agents were tested at concentrations equivalent to 10× and 100× EC_{50}, producing similar results. Assay plates were kept in a humidified 37-°C incubator before and after drug–medium additions. Plates were developed 48 h.p.i. using ONE-Glo Luciferase Assay reagent (Promega) and the resulting luminescence data were collected and analysed using EnVision Manager 1.13.3009 and GraphPad Prism 7.0 software, respectively. When investigating inhibitor potency across the phases of viral replication, single-cycle antiviral assays were performed in MT-2 cells in a manner such that GS-6207 was present selectively at early stage, late stage or during a full course of infection as previously described[34]. Assays evaluating the effect of GS-6207 on HIV-1 particle production (by p24 antigen enzyme-linked immunosorbent assay) and intracellular CA levels (by anti-p24 and anti-tubulin western blot analyses) have previously been described[21].

For in vitro two-drug combination studies, compounds within a test pair were combined in 384-well assay plates to create a two-dimensional matrix of diluted drugs. Positive control (EVG) and negative control (DMSO) wells were included in every assay plate to define 100% and 0% protection from viral replication-mediated cytopathic effect (CPE), respectively. The final DMSO concentration in the assay was 0.5%. MT-2 cells were bulk-infected in complete RPMI medium with HIV-1 strain IIIB at a multiplicity-of-infection (MOI) of 0.01 for 3 h at 37 °C, added to the assay plates (3×10^3 cells per well) and incubated at 37 °C for 5 days. Cell viability was determined by adding CellTiter-Glo reagent and the resulting luminescence data were collected using EnVision Manager 1.13.3009. Data were normalized to positive and negative controls in each plate, expressed as per cent CPE protection and analysed with MacSynergy II software[35]. Combination data were analysed at the 95% confidence level, with synergy and antagonism volumes defined as follows: high synergy (>100 μM^2%), moderate synergy (50 to <100 μM^2%), additivity (>-50 to <50 μM^2%) and antagonism (<-50 μM^2%).

Antiviral assays using HIV-1 strain BaL in primary human CD4$^+$ T lymphocytes and macrophage cultures were conducted using a p24 endpoint assay as previously described[36]. A seven-day reverse transcriptase endpoint antiviral assay using fresh human PBMCs independently infected with a panel of clinical HIV-1 and HIV-2 isolates was performed by Southern Research as a contracted research study.

Cytotoxicity assays

For cytotoxicity assessment in MT-4 cells, PBMCs, primary human CD4$^+$ T cells and monocyte-derived macrophages, the protocol was identical to that of the respective antiviral assay, including assay duration, except that no virus was added to the plates. Protocols for cytotoxicity assessments in Huh-7, Gal-HepG2, Gal-PC-3 and MRC-5 cell lines, as well as in primary human hepatocytes, have previously been described[37]. The effect of test compounds on cell viability was measured using CellTiter-Glo. Data analysis was performed using GraphPad Prism 7.0 to calculate CC_{50} values.

GS-6207 resistance analysis

Dose-escalation selections for drug-resistant HIV-1 variants were performed in MT-2 cells infected with HIV-1 strain HXB2D using twofold incremental increases in GS-6207 concentration as previously described[31]. The resistance profile of each emergent virus passage was then assessed in the five-day cytoprotection antiviral MT-2 assay after titrating virus inoculums to normalize the MOI across all samples. Viral breakthrough selections were conducted under conditions of fixed, constant drug concentrations over a period of 35 days in human PBMCs independently infected with 6 different HIV-1 isolates (BaL, 92US657, 91US0006, 7406, 7467 and 7576) as previously described[21]. GS-6207 was tested at fixed drug concentrations equal to 4-fold, 8-fold and 16-fold its EC_{95} value of 0.23 nM (0.92 nM, 1.9 nM, and 3.7 nM GS-6207, respectively), using 6 replicate cell cultures per experimental condition. Viruses that emerged in the presence of GS-6207 were genotyped by population sequencing. Total RNA was isolated from mock- and GS-6207-selected virus-containing supernatants using the QiaAMP Viral RNA Mini Kit (Qiagen). A 986-bp fragment encoding HIV-1 capsid and the adjacent p2 spacer peptide was amplified by PCR with reverse transcription (RT–PCR) using the Qiagen OneStep RT–PCR Kit in combination with primers 5′-CAGTAGCAACCCTCTATTGTGTGC-3′ and 5′-CCTAGGGGCCCTGCAATTT-3′. RT–PCR products were sequenced by Elim Biopharmaceuticals. To identify codon changes, gene sequences from selected HIV-1 variants were aligned using DNA Sequencher 4.9 Software (Gene Codes) with that of the input virus and virus passaged in the absence of GS-6207. For samples containing >1 codon change, PCR products were subcloned, DNA was isolated from individual bacterial colonies and the gene encoding CA was sequenced to assess the linkage of all observed substitutions.

The resistance profile and infectivity of each GS-6207-selected CA variant was determined in MT-2 cells after introducing each substitution, alone and in combination, into wild-type single-cycle reporter HIV-1. The replication level (fitness) of select CA variants introduced into wild-type replication-competent reporter HIV-1 was evaluated in primary human CD4$^+$ T cells over a period of 19 days[21].

Recombinant HIV-1 Gag and CAs

Recombinant HIV-1_{LAI} CA was prepared as previously described[38]. Soluble cross-linked CA hexamers of HIV-1 strain NL4.3 (wild type and the M66I variant), as well as CA pentamers, were prepared as previously described[38–40]. Recombinant Gag protein of HIV-1 strain NL4.3 was prepared as previously described[21].

Crystallization, data collection and structure determination

HIV-1 CA hexamer (25 mg ml^{-1} in 20 mM Tris, pH 8.0) was thawed and diluted to 12 mg ml^{-1} in the same buffer and incubated on ice for 10 min with 1 mM GS-6207. Crystallization droplets were assembled in MRC2 microplates with 100 nl of the complex and 100 nl of 12% polyethylene glycol (PEG) 3350, 0.2 M sodium thiocyanate, 0.1 M sodium cacodylate, pH 6.7. The assembled 200-nl droplet was then subjected to vapour diffusion with 50 µl of 1% PEG 3350, 0.2 M sodium thiocyanate, 0.1 M sodium cacodylate, pH 6.7 in the large reservoir. Large hexagonal crystals (30 µm × 160 µm × 160 µm) grew in 4 d at 25 °C and were subsequently cryo-protected for X-ray diffraction in 30% PEG 3350, 7% glycerol, 0.2 M sodium thiocyanate, 0.1 M sodium cacodylate, pH 6.7, and 0.3 mM GS-6207. X-ray diffraction data to 2.0 Å resolution were collected on a single frozen (−180 °C) crystal at the Advanced Light Source, Beamline 5.0.1. The protein–inhibitor complex crystallized in space group P3 with cell parameters: a = 158.3 Å, b = 158.3 Å, c = 55.6 Å, α = 90.0°, β = 90.0° and γ = 120.0°. The data were processed and scaled with the programs DENZO and SCALEPACK (HKL Research), respectively. Initial models were obtained by molecular replacement using the program EPMR[41] and using the coordinates from a single monomer of a previously determined HIV-1 CA hexamer–inhibitor complex (with coordinates for the inhibitor atoms removed) as the search model. The molecular replacement solution included six monomers. The initial model was further refined using multiple rounds of simulated annealing in the PHENIX software package[42] followed by manual refitting of the model in COOT[43]. In the later stages of refinement, strong residual electron density in the capsid modulator binding site allowed for unambiguous placement of GS-6207 into the structure followed by final refinement of the model (see Supplementary Fig. 2 for sample inhibitor density). Data collection and model refinement statistics are summarized in Extended Data Table 4.

In vitro HIV-1 CA assembly assay

The in vitro assembly of HIV-1 CA in the presence and absence of small-molecule library compounds (10 µM) or twofold serially diluted GS-6207 was monitored by measuring changes in sample absorbance over time at 350 nm. Final assembly reactions contained 20 µM CA, 2 M NaCl, 50 mM sodium phosphate pH 7.5, 0.005% Antifoam 204 (Sigma-Aldrich) and 1% DMSO. Sample absorbance values at 350 nm were monitored over time at 25 °C in 96-well or 384-well plates using an M5 plate reader (Molecular Devices), corrected for absorbance values in the absence of CA or NaCl, and the data analysed using SoftMax Pro 6.3.1 as previously described[38].

GS-6207 binding assay

Surface plasmon resonance biosensor binding experiments were performed using the ProteOn XPR36 platform (CA hexamer and pentamer proteins) or the Biacore T100 platform (CA monomer and Gag proteins) as previously described[21]. Data were analysed using ProteOn Manager 3.1.0 or Scrubber 2.0 and fit with a simple kinetic model with a term for mass transport added when necessary.

Quantification of HIV-1 DNA

MT-2 cells (2×10^6 cells ml^{-1}) were infected with single-cycle reporter HIV-1, added to 24-well plates containing drug medium and transferred to a humidified 37-°C incubator. For each condition, cells from each of 3 replicate wells were collected at 12 h.p.i. for late reverse transcription product quantification, 24 h.p.i. for 2-LTR circle quantification, and 48 h.p.i. for Alu-LTR product quantification. Viral DNA was isolated from cell pellets using a QIAamp DNA mini kit (Qiagen) and quantified using the TaqMan real-time PCR and ABI Prism 7900HT sequence detection system (Applied Biosystems) or the QX200 Droplet Digital PCR System (Bio-Rad) as previously described[21].

Ultrastructural analysis of HIV-1 by electron microscopy

MT-2 cells infected with HIV-1 strain IIIB were washed and cultured at 37 °C in complete RPMI containing 0.25% DMSO, 15 nM GS-6207 or 500 nM ATV. After a four-day incubation, samples were pelleted, fixed, stained, sectioned and imaged on a JEOL JEM-1230 transmission electron microscope as previously described[21].

Metabolic stability of [^{3}H]GS-6207 in primary human hepatocytes

A 500-µl suspension of human hepatocytes (1×10^6 cells ml^{-1}) and 0.25 µM [^{3}H]GS-6207 was prepared in Krebs–Henseleit Buffer (KHB) medium and incubated in a humidified 37-°C incubator with 5% CO_2 in duplicate wells of a 24-well plate. Propranolol (1 µM final), a compound known to be efficiently metabolized by hepatocytes by oxidation and conjugation, was used as a positive control. A cell-free control was incubated in parallel as a negative control. Aliquots (100 µl) were removed after 0, 1, 3 and 6 h, mixed with 200 µl quenching solution, placed on a shaker for 10 min and then centrifuged at 3,000*g* for 60 min. The supernatant was transferred to a new plate, diluted with 100 µl water and placed on a shaker for 10 min. The quantification of [^{3}H]GS-6207 and its metabolites was performed by radio flow chromatography using a Perkin Elmer Radiomatic 625TR flow scintillation analyser with a 500 µl flow cell coupled to a Dionex Ultimate 3000 HPLC system. The scintillation cocktail was Perkin Elmer Ultima-Flo and was mixed with the HPLC effluent at a ratio of 1:1. The sample (100 µl) was injected with a Leap Technologies CTC PAL autosampler. Separation was achieved on a Phenomenex Synergi Fusion-RP 80 Å pore size, 4-µm particle size, 150 × 4.6-mm column maintained at 32 °C. Mobile phase A consisted of 95% water, 5% acetonitrile, and contained 0.1% trifluoroacetic acid (TFA). Mobile phase B consisted of 95% acetonitrile, 5% water, and contained 0.1% TFA. Elution was achieved, at a flow rate of 1 ml min^{-1}, by linear gradients: initial condition was 2% B at 0 min which was increased to 75% B over 45 min, holding for 4 min at 75% B and then returning to initial conditions. The column was allowed to re-equilibrate for 12 min between injections. Quantification was by radiochromatographic peak area.

Competitive equilibrium dialysis

Human serum protein binding to GS-6207 was determined by competitive equilibrium dialysis. Human plasma (10%) was spiked with GS-6207 (2 µM) and blank RPMI cell culture medium containing 2% FBS were placed in duplicate into opposite sides of assembled dialysis cells. After a 24-h equilibration period at 37 °C, GS-6207 concentrations in plasma and cell culture medium were determined by a liquid chromatography with tandem mass spectrometry (LC–MS/MS) method and multiplied by 10 to obtain the protein-adjusted shift for 100% human plasma.

Ethical conduct and consent in clinical trials

The clinical trials were conducted in accordance with Good Clinical Practice, as defined by the International Conference on Harmonization and in accordance with the ethical principles underlying the United States Code of Federal Regulations, Title 21, Part 50 (21CFR50). The protocol and the participant informed-consent form received institutional review board, independent ethics committee approval and/or favourable opinion (Advarra) before initiation of the study. Freely given written informed consent was obtained from every individual before participation in the clinical studies.

Single ascending-dose study in healthy participants

For clinical study GS-US-200-4070, we enrolled healthy men and women uninfected with HIV-1, 18–45 years of age, with normal kidney and liver function, body mass index between 19 and 30 kg/m^2, and no relevant medical history. Ten trial participants in each dosing arm were randomized in a blinded fashion in a 4:1 ratio to receive either the drug (GS-6207) or placebo (vehicle alone). The primary objectives were to assess the safety and tolerability of escalating single subcutaneous doses of GS-6207 compared with placebo in healthy participants and to assess its pharmacokinetics. GS-6207 was formulated as a sterile, preservative-free, injectable aqueous suspension (100 mg m1^{-1}). Serial blood samples were collected for plasma pharmacokinetics analysis through day 197 (30- and 100-mg cohorts) or day 225 (300- and 450-mg cohorts). Plasma samples were analysed using a validated, high-performance LC–MS/MS bioanalytical method with multiple reaction monitoring and electrospray ionization in the positive mode (Covance Laboratories). Quantification was performed using multiple reaction monitoring of the transitions *m/z* 968.2 to 869.2 and *m/z* 974.3 to 875.2 for GS-6207 and an isotopically labelled internal standard, respectively. The bioanalytical method was validated over a calibrated range of 0.5 to 500 ng ml^{-1}. Inter-assay precision, based on coefficient of variation, was ≤ 8.7%, and accuracy ranged from 95.2% to 104.6%. All plasma samples were analysed within the timeframe supported by frozen stability storage data. Pharmacokinetic parameters were estimated using Phoenix WinNonlin 6.4 (Certara, L.P.) software using standard noncompartmental methods. Pharmacokinetics parameters for GS-6207 included area under plasma concentration versus time curve extrapolated to infinity (AUC_{inf}), the per cent of the area that is extrapolated ($AUC_{\%exp}$), and area under the concentration versus time curve from time zero to the last quantifiable concentration (AUC_{last}), maximal concentration (C_{max}), time to C_{max} (t_{max}) and $t_{1/2}$.

Single ascending-dose study in participants living with HIV

For clinical study GS-US-200-4072 (registered with ClinicalTrials.gov, NCT03739866), we enrolled treatment-naive or -experienced, but HIV-capsid-inhibitor-naive and integrase-strand-transfer-inhibitor-naive, men and women, 18–65 years of age with plasma HIV-1 RNA ≥ 5,000 copies ml^{-1} (via amendment; originally 10,000 copies ml^{-1}) but ≤ 400,000 copies ml^{-1} and CD4$^+$ T cell counts >200 cells per mm^3. Eight trial participants in each dosing arm were randomized in a 3:1 ratio to receive either the drug (GS-6207) or placebo (vehicle alone) (part A). GS-6207 was formulated as a sterile, preservative-free, injectable aqueous suspension (100 mg m1^{-1}).

Plasma HIV-1 RNA levels were determined using the Roche COBAS Ampliprep/COBAS TaqMan HIV-1 test v.2, which has a limit of detection of 20 copies ml^{-1} and a range of quantification of 20 to 10,000,000 HIV-1 RNA copies ml^{-1}. All samples were analysed by a central laboratory. Serial blood samples were collected for plasma pharmacokinetics through at least day 9. Pharmacokinetics samples were analysed as above for study 200-4070.

HIV-1 resistance analyses for study GS-US-200-4072 were carried out at Monogram Biosciences using the research-grade gag-protease genotyping (population-level sequencing) and phenotyping assay to assess resistance to GS-6207 using HIV-1 DNA fragment of each participant that encompasses the gag-protease HIV-1 region, and/or using the CLIA-certified PhenoSense GT + Integrase or GenoSure PRIme assay to assess resistance to the components of Biktarvy (which was administered to all participants following the 9-day GS-6207 monotherapy). Resistance analyses were conducted at screening and day 9 (last GS-6207 monotherapy visit).

Within part A, we conducted an interim analysis, which was prespecified in the protocol to be conducted after at least 50% of the participants and/or after all participants within each cohort completed the day-10 visit. The purpose of this interim analysis was to select the doses of GS-6207 to evaluate in each subsequent cohort.

Statistics

GraphPad Prism 7.0 was used for statistical analysis. In each case, an unpaired two-tailed Student's *t*-test with Welch's correction was performed for parametric analysis of two groups. A P value < 0.05 was considered statistically significant.

Reporting summary

Further information on research design is available in the Nature Research Reporting Summary linked to this paper.

Data availability

All data to understand and assess the conclusions of this research are available in the Article and Supplementary Information. Raw gel source

data for Fig. 2f are available in Supplementary Fig. 1. Small-molecule X-ray crystallographic coordinates and structure factor files have been deposited in the Protein Data Bank (PDB) with accession number 6V2F. Study GS-US-200-4072 was registered with ClinicalTrials.gov, NCT03739866. The datasets generated during and/or analysed during the current study are available from the corresponding author on reasonable request.

31. Tsiang, M. et al. Antiviral activity of bictegravir (GS-9883), a novel potent HIV-1 integrase strand transfer inhibitor with an improved resistance profile. *Antimicrob. Agents Chemother.* **60**, 7086–7097 (2016).
32. Margot, N. A., Gibbs, C. S. & Miller, M. D. Phenotypic susceptibility to bevirimat in isolates from HIV-1-infected patients without prior exposure to bevirimat. *Antimicrob. Agents Chemother.* **54**, 2345–2353 (2010).
33. Nakabayashi, H., Taketa, K., Miyano, K., Yamane, T. & Sato, J. Growth of human hepatoma cells lines with differentiated functions in chemically defined medium. *Cancer Res.* **42**, 3858–3863 (1982).
34. Balakrishnan, M. et al. Non-catalytic site HIV-1 integrase inhibitors disrupt core maturation and induce a reverse transcription block in target cells. *PLoS ONE* **8**, e74163 (2013).
35. Prichard, M. N. & Shipman, C. Jr. Analysis of combinations of antiviral drugs and design of effective multidrug therapies. *Antivir. Ther.* **1**, 9–20 (1996).
36. Bam, R. A. et al. TLR7 agonist GS-9620 is a potent inhibitor of acute HIV-1 infection in human peripheral blood mononuclear cells. *Antimicrob. Agents Chemother.* **61**, e01369-16 (2016).
37. Warren, T. K. et al. Therapeutic efficacy of the small molecule GS-5734 against Ebola virus in rhesus monkeys. *Nature* **531**, 381–385 (2016).
38. Hung, M. et al. Large-scale functional purification of recombinant HIV-1 capsid. *PLoS ONE* **8**, e58035 (2013).
39. Pornillos, O. et al. X-ray structures of the hexameric building block of the HIV capsid. *Cell* **137**, 1282–1292 (2009).
40. Pornillos, O., Ganser-Pornillos, B. K. & Yeager, M. Atomic-level modelling of the HIV capsid. *Nature* **469**, 424–427 (2011).
41. Kissinger, C. R., Gehlhaar, D. K. & Fogel, D. B. Rapid automated molecular replacement by evolutionary search. *Acta Crystallogr. D* **55**, 484–491 (1999).
42. Adams, P. D. et al. PHENIX: a comprehensive Python-based system for macromolecular structure solution. *Acta Crystallogr. D* **66**, 213–221 (2010).
43. Emsley, P., Lohkamp, B., Scott, W. G. & Cowtan, K. Features and development of Coot. *Acta Crystallogr. D* **66**, 486–501 (2010).

Acknowledgements We thank D. Cowfer, K. Brendza, G. Czerwieniec, M. Tsiang, K. Wang, G. Lane, M. Kenney, M. Ceo, S. Kazerani, T. Lane, L. Meng, T. Rainey, A. Vandehey, A. Wagner, M. O'Keefe, J. Yoon, S. Neville, W. Lew, B. Ross, Q. Wang, J. Cha, M. Tran and K. Nguyen for their support and contributions, and all the people who participated in the phase-I clinical trials, including the study participants, their families, and the principal investigators and their staff.

Author contributions T.C. conceived the project. D.J., M.H. and N.N. conducted protein purifications, and X.L. and R.S. oversaw the analysis. S.R.Y., N.P., T.Z.C., D.K. and L.L designed, conducted and analysed small-molecule library screens. T.C., J.O.L., S.R.Y., R.L.H., W.C.T., M.S.R. and A.E.C. provided project leadership. J.O.L., W.C.T., S.D.S., C.-H.C., E.C., G.B., J.R.Z., J. Li, M.G., P.M., Q.L., Q.W., R.L.H., R.D.S., S.D.S., S.E.L. and S.B. were responsible for the design, synthesis, characterization and scaling-up of small molecules. A.N.-M. conducted and analysed in vitro CA assembly assays. S.R.Y. and A.N.-M. conducted and analysed virion morphology by electron microscopy. G.J.S., S.A. and H.Y. designed, conducted and analysed high-throughput antiviral measurements. G.J.S, S.A., A.M. and Y.X. conducted cell-based assays for cytotoxicity. G.J.S. conducted and analysed in vitro drug combination studies. A.M. and R.R.R. conducted and analysed in vitro antiviral testing against HIV mutants with resistance to existing agents. A.G.V. and R.L.A. conducted protein crystallization studies, J.R.S. collected and analysed X-ray crystallographic data, and T.C.A. prepared the refinement table. C.E.C. and E.Y.H. conducted structural modelling studies to guide small-molecule development. G.A.P., M.H.W., S.A.L., S.C. and L.L. conducted and analysed biosensor binding studies. S.R.Y. A.M., E.S. and L.K.T. conducted and analysed cell-based mechanism-of-action studies. A.L. conducted and analysed biochemical protease assays. A.M., D.H., R.A.B. and S.R.Y. conducted resistance selection assays and characterized emergent HIV-1 CA variants. J.Z., B.L. and J.M. designed and executed preclinical pharmacokinetics and metabolism studies, and summarized results. A.E.C. oversaw all anatomical pathology examinations and analyses of preclinical animal species. W.R., S. Sellers and A.C. designed and tested drug formulations. A.C. and S.A.W. oversaw GS-6207 chemistry, manufacture and control for clinical studies. M.S.R., R.H., R.B. and D.M.B. designed and supervised the clinical studies, and G.I.S., P.J.R., G.E.C., C.K.M. and E.S.D conducted them. R.B., J. Ling, Y.-P. L., N.M. and C.C. conducted and coordinated clinical sample and statistical analyses. W.I.S. provided project guidance during the early discovery phase, and S. Swaminathan and W.E.L. provided long-term project oversight. S.R.Y., M.S.R., J.O.L. and T.C. wrote the manuscript, with input from all authors.

Competing interests All authors are current or previous employees of Gilead Sciences (except for G.I.S., P.J.R., G.E.C., C.K.M., W.I.S. and E.S.D.) and received salary and stock ownership as compensation for their employment. M.G., J.O.L., W.R., R.D.S., S.D.S., W.C.T. and J.R.Z. are inventors on granted US patent no. 10,071,985B2 covering GS-6207 composition of matter and methods of use. G.I.S. receives research support from Gilead Sciences, Janssen Pharmaceutica, GlaxoSmithKline, Abbvie and Cepheid, and is on the speaker's bureau and advisory board for Janssen, ViiV Healthcare and Merck. G.E.C. receives grants (investigator research payments) from Gilead Sciences, ViiV Healthcare, Merck and Janssen Pharmaceutica. C.K.M. receives research support from Gilead Sciences, Merck, ViiV Healthcare and Janssen Pharmaceutica, is on the speaker's bureau for Gilead Sciences, Merck and Insmed, and is on an advisory board for Gilead Sciences. E.S.D. receives research support from Gilead Sciences, Merck and ViiV Healthcare, and has served as a consultant for Gilead Sciences.

Additional information

Supplementary information is available for this paper at https://doi.org/10.1038/s41586-020-2443-1.
Correspondence and requests for materials should be addressed to S.R.Y.
Peer review information *Nature* thanks Daniel R. Kuritzkes, Kevan Shokat and the other, anonymous, reviewer(s) for their contribution to the peer review of this work.
Reprints and permissions information is available at http://www.nature.com/reprints.

Extended Data Table 1 | Cytotoxicity of GS-6207 in human cell lines and primary cells

	CC_{50} (μM)	
	GS-6207	**Puromycin**
Human cell lines		
MT-4	24.7 ± 18.3	0.2 ± 0.1
Huh-7	>44.4	0.5 ± 1.7
Gal-HepG2	>44.4	1.0 ± 1.7
Gal-PC-3	>44.4	0.4 ± 1.5
MRC-5	>44.4	0.3 ± 1.5
Human primary cells		
Hepatocytes	>50.0	1.6 ± 0.6
Quiescent PBMCs	>44.4	0.6 ± 1.5
Stimulated PBMCs	>50.0	0.2 ± 0.1
$CD4^+$ T-lymphocytes	>50.0	0.2 ± 0.1
Monocyte-derived macrophages	>50.0	4.5 ± 2.8

Data are mean ± s.d. from 3 independent experiments (n = 4 biological replicates each). Puromycin was assayed in parallel as a positive control for cytotoxicity.

Extended Data Table 2 | In vitro combination studies with GS-6207

	TAF	EFV	DTG	DRV	GS-6207
Synergy volume [$\mu M^2.\%$]	87 ± 32	101 ± 40	116 ± 13	119 ± 39	18 ± 8
Antagonism volume [$\mu M^2.\%$]	-8 ± 7	-8 ± 8	-8 ± 7	-3 ± 3	-16 ± 6
Combination effect	Moderately synergistic	Highly synergistic	Highly synergistic	Highly synergistic	Additive

TAF is a nucleotide reverse transcriptase inhibitor; EFV is a nonnucleoside reverse transcriptase inhibitor; DTG is an integrase strand transfer inhibitor); DRV is an HIV protease inhibitor; GS-6207 in combination with itself was included as a positive control for additivity. Data are mean ± s.d. from 3 independent experiments (n = 3 biological replicates each). The high-antagonism control combination of ribavirin and stavudine produced the expected results (synergy volume = 0 ± 0; antagonism volume = −398 ± 23).

Extended Data Table 3 | GS-6207 activity against HIV-1 isolates that are resistant to existing antiretroviral inhibitors

		Fold resistance (*n*)		
Antiretroviral Class	**HIV-1 Mutant**	**GS-6207**	**Control Antiretroviral Agent**	
Nucleotide reverse transcriptase inhibitor (NRTI)	K65R	0.6 ± 0.2 (3)	FTC	14.1 ± 2.6 (3)
	M184V	0.3 ± 0.3 (3)	FTC	>23.0 (3)
	6TAMs	0.2 ± 0.1 (3)	FTC	4.0 ± 2.8 (3)
Nonnucleoside reverse transcriptase inhibitor (NNRTI)	Y188L	0.5 ± 0.1 (3)	EFV	>22.5 (3)
	L100I+K103N	0.5 ± 0.2 (3)	EFV	>22.5 (3)
	K103N+Y181C	0.6 ± 0.2 (3)	EFV	>22.5 (3)
Integrase strand transfer inhibitor (INSTI)	E138K+Q148K	0.6 ± 0.3 (3)	EVG	>53.8 (3)
	G140S+Q148R	0.8 ± 0.3 (3)	EVG	>53.8 (3)
	E92Q+N155H	0.8 ± 0.4 (3)	EVG	>53.8 (3)
	N155H+Q148R	1.2 ± 0.7 (3)	EVG	>52.9 (3)
Maturation inhibitor (MI)	V230I in CA	0.7 ± 0.2 (6)	BVM	>67.5 (6)
	V7A in SP1	0.8 ± 0.4 (8)	BVM	>67.5 (7)
Protease inhibitor (PI)	M46I+I50V	0.7 ± 0.2 (3)	DRV	27.1 ± 23.1 (3)
	I84V+L90M	0.3 ± 0.1 (3)	ATV	32.7 ± 7.8 (3)
	G48V+V82A+L90M	0.5 ± 0.2 (3)	ATV	31.0 ± 11.9 (3)
	G48V+V82S	0.4 ± 0.2 (3)	ATV	15.2 ± 3.2 (3)

SP1, 14-amino-acid spacer peptide 1, located between CA and nucleocapsid (NC) in HIV-1 Gag; 6TAMs, six non-polymorphic HIV-1 reverse-transcriptase mutations (M41L, D67N, K70R, L210W, T215Y and K219Q) that confer resistance to thymidine analogues. Data are geometric mean ± s.d. from three biological replicates in each of at least three independent experiments (exact *n* given in parentheses).

Extended Data Table 4 | Data collection and refinement statistics (molecular replacement)

	HIV-1 Capsid hexamer - GS-6207 complex
Data collection	
Space group	P3
Cell dimensions	
a, *b*, *c* (Å)	158.30, 158.30, 55.65
α, β, γ (°)	90, 90, 120
Resolution (Å)	30.00 - 2.00 (2.07 - 2.00) *
R_{sym} or R_{merge}	0.119 (0.795)
$I / \sigma I$	18.80 (1.94)
Completeness (%)	98.66 (90.82)
Redundancy	5.2 (4.3)
Refinement	
Resolution (Å)	29.18 - 2.00 (2.07 - 2.00)
No. reflections	105,864 (9,768)
R_{work} / R_{free}	0.2051 / 0.2492 (0.2447 / 0.2712)
No. atoms	
Protein	9,456
Ligand/ion	384
Water	896
B-factors	
Protein	30.72
Ligand/ion	25.60
Water	38.83
R.m.s. deviations	
Bond lengths (Å)	0.003
Bond angles (°)	0.570
Ramachandran statistics	
Favored (%)	99.40
Allowed (%)	0.60
Outliers (%)	0.00
Rotamer outliers	0.00

All data were collected from a single crystal. For inhibitor electron density defined by X-ray crystallography, see Supplementary Fig. 2.
*Values in parentheses are for the highest-resolution shell.

Extended Data Table 5 | Biosensor surface-plasmon-resonance assays of GS-6207 binding to recombinant CA

	Immature capsid	Mature capsid			
	Gag polyprotein	CA monomer	CA pentamer	CA hexamer	CA hexamer_M66I
K_D (pM)	1,100 ± 900	2,500 ± 500	220 ± 160	240 ± 90	60,000 ± 20,000
k_{on} ($M^{-1}s^{-1}$)	ND	ND	$2 \pm 1 \times 10^5$	$6.5 \pm 0.3 \times 10^4$	$6 \pm 4 \times 10^4$
k_{off} (s^{-1})	ND	ND	$2.7 \pm 0.4 \times 10^{-5}$	$1.4 \pm 0.4 \times 10^{-5}$	$2.6 \pm 0.3 \times 10^{-3}$

M66I is an in vitro GS-6207-selected CA binding-site mutant that confers high-level resistance to GS-6207. ND, not determined (because the binding rate was too fast to be determined reliably). Data are mean ± s.d. from four independent experiments (or three for the M66I variant), assayed in singlet.

Extended Data Table 6 | Resistance profile of HIV-1 CA mutants identified in viruses selected by GS-6207

HIV-1 CA Sequence	WT	Q67H	N74D	K70N	Q67H N74S	Q67H T107N	L56I	Q67H N74D	M66I
Mean EC_{50} (pM) in MT-2 cells *	31	196	682	741	996	1,910	7,400	34,069	>100,000
Fold GS-6207 resistance †	1	6	22	24	32	62	239	1,099	>3,226
Infectivity (% WT) in a single-cycle replication assay in MT-2 cells ‡	100	95	48	7	34	41	9	29	6
Peak replication level (% WT) in primary human $CD4^+$ T-cells infected with a replication-competent reporter HIV-1 §	100	100	1	1	69	28	3	<1	<1

*Data are mean single-cycle EC_{50} values from 3 independent experiments (n = 3 biological replicates each).

†Data are mean EC_{50} ratios of mutant to wild type, from 3 independent experiments (n = 3 biological replicates each).

‡Data are mean luminescence values expressed as a percentage of those of the wild-type virus, from 3 independent experiments (n = 3 biological replicates each).

§Data are mean luminescence values expressed as a percentage of those of the wild-type virus from 2 independent experiments (n = 6 biological replicates each).

Extended Data Table 7 | Baseline characteristics and clinical adverse events in healthy participants (that affected >1 participant overall) in study GS-US-200-4070

	GS-6207					
Baseline characteristics	**30 mg (*n* = 8)**	**100 mg (*n* = 8)**	**300 mg (*n* = 8)**	**450 mg (*n* = 8)**	**Placebo (*n* = 8)**	**Overall (*n* = 40)**
Age, years, median (range)	40 (29-43)	36 (19-42)	34 (22-41)	36 (27-42)	41 (21-44)	37 (19-44)
Sex at birth: female, n (%)	3 (38)	5 (63)	3 (38)	1 (13)	1 (13)	13 (33)
Race: black, n (%)	3 (38)	2 (25)	1 (13)	3 (38)	2 (25)	11 (28)
Body mass index, kg/m^2, median (range)	28 (23-30)	26 (21-29)	24 (23-30)	28 (23-30)	27 (21-30)	26 (21-30)
Safety: preferred term						
Any AE, n (%)	4 (50)	8 (100)	7 (88)	6 (75)	4 (50)	29 (73)
Injection site erythema	1 (13)	5 (63)	6 (75)	3 (38)	0	15 (38)
Injection site pain	0	3 (38)	6 (75)	3 (38)	2 (25)	14 (35)
Injection site nodule	0	5 (63)	3 (38)	1 (13)	0	9 (23)
Injection site induration	0	0	6 (75)	2 (25)	0	8 (20)
Injection site swelling	1 (13)	5 (63)	1 (13)	0	0	7 (18)
Headache	2 (25)	1 (13)	2 (25)	0	0	5 (13)
Injection site pruritus	1 (13)	0	1 (13)	1 (13)	0	3 (8)
Viral upper respiratory tract infection	0	0	0	2 (25)	1 (13)	3 (8)
Acne	0	0	0	2 (25)	0	2 (5)
Back pain	0	0	2 (25)	0	0	2 (5)
Dizziness	0	0	1 (13)	1 (13)	0	2 (5)
Injection site bruising	0	0	1 (13)	0	1 (13)	2 (5)
Nausea	1 (13)	0	1 (13)	0	0	2 (5)
Oropharyngeal pain	1 (13)	0	0	0	1 (13)	2 (5)
Skin mass	0	0	1 (13)	1 (13)	0	2 (5)

AE, adverse event.

Extended Data Table 8 | Baseline characteristics and clinical serious adverse events (that affected any participant) and adverse events (that affected >1 participant overall) in participants living with HIV in study GS-US-200-4072

Baseline characteristics	GS-6207 20 mg or Placebo (*n* = 8)	GS-6207 50 mg or Placebo (*n* = 8)	GS-6207 150 mg or Placebo (*n* = 8)	GS-6207 450 mg or Placebo (*n* = 8)
Age, years, median (range)	35 (23-50)	28 (19–56)	36 (24–56)	29 (20–59)
Sex at birth: female, n (%)	1 (13)	0	1 (13)	0
Race: black, n (%)	2 (25)	2 (25)	3 (38)	3 (38)
Body mass index (kg/m^2), median (range)	25 (21-38)	25 (21–28)	26 (20–34)	25 (23–29)
HIV-1 RNA, log_{10} copies ml^{-1}, median (range)	4.47 (3.86-5.01)	4.33 (4.01-4.85)	4.57 (4.15-4.92)	4.48 (4.31-4.84)
CD4 count, cells μl^{-1}, median (range)	472 (217-574)	594 (362-1009)	388 (294-800)	430 (200-968)
ARV treatment naïve, n (%)	8 (100)	6 (75)	4 (50)	7 (88)
Median duration of follow up, Days (range)*	38 (17 to 73)	129 (122 to 136)	199 (164 to 199)	122 (113 to 136)
Safety: Preferred term				
Serious AE, n (%)				
Atrial fibrillation	0	0	0	1 (13)†
Any AE, n (%)	5 (63)	6 (75)	7 (88)	6 (75)
Injection site pain	0	4 (50)	5 (63)	4 (50)
Injection site erythema	1 (13)	1 (13)	5 (63)	2 (25)
Injection site induration	0	1 (13)	4 (50)	2 (25)
Injection site nodule	0	1 (13)	1 (13)	2 (25)
Upper respiratory tract infection	0	0	0	4 (50)
Headache	1 (13)	0	1 (13)	1 (13)
Nausea	2 (25)	1 (13)	0	0
Oropharyngeal pain	1 (13)	1 (13)	0	1 (13)
Vomiting	2 (25)	1 (13)	0	0
Arthralgia	0	0	2 (25)	0
Constipation	0	1 (13)	0	1 (13)
Haemorrhoids	0	1 (13)	0	1 (13)
Nasopharyngitis	0	0	2 (25)	0
Rash	1 (13)	1 (13)	0	0
Syphilis	0	1 (13)	0	1 (13)

*All participants were administered the components of Biktarvy (bictegravir, emtricitabine, and tenofovir alafenamide) after nine days of GS-6207 monotherapy.
†One participant who received either 450 mg GS-6207 or placebo experienced a serious adverse event of atrial fibrillation on day 113, while receiving Biktarvy, after amphetamine use.

Extended Data Table 9 | Clinical pharmacokinetic parameters in healthy volunteers and participants living with HIV

	GS-6207 in Healthy Volunteers					GS-6207 in PLWH			
Parameter	**30 mg (*n* = 8)**	**100 mg (*n* = 8)**	**300 mg (*n* = 8)**	**450 mg (*n* = 8)**	**Parameter**	**20 mg (*n* = 6)**	**50 mg (*n* = 6)**	**150 mg (*n* = 6)**	**450 mg (*n* = 6)**
AUC_{inf} ($hr*ng\ ml^{-1}$)	8,700 (27.1)	27,300 (41.5)	86,100 (18.3)	108,000 (24.4)	C_{D9} ($ng\ ml^{-1}$)	2.58 (41.5)	4.40 (89.9)	12.9 (39.3)	38.2 (35.1)
AUC_{last} ($hr*ng\ ml^{-1}$)	5,500 (42.2)	23,600 (45.1)	73,100 (35.4)	97,600 (29.9)	C_{D9} / $paEC_{95}$ (mean)	0.67	1.14	3.33	9.87
AUC_{exp} (%)	17.6 (69.4)	6.78 (65.0)	5.39 (126)	3.29 (69.9)					
C_{max} ($ng\ ml^{-1}$)	3.2 (39.8)	14.7 (58.4)	47.9 (27.7)	58.4 (39.2)					
T_{max} (day)	35.0 (16.5, 38.5)	21.0 (9.50, 39.0)	31.5 (14.0, 35.0)	14.0 (6.00, 31.5)					
$T_{1/2}$ (day)	37.0 (32.8, 46.2)	31.9 (21.3, 48.2)	45.4 (26.6, 62.5)	39.7 (29.7, 48.7)					

Data are shown to three significant figures and are presented as mean (per cent coefficient of variation), except for T_{max} and $t_{1/2}$, which are median (with first and third quartiles in parentheses). PLWH, people living with HIV; C_{D9}, GS-6207 plasma concentration on day 9; C_{D9}/protein-adjusted (pa)EC_{95} = fold EC_{95} coverage on day 9.

Extended Data Table 10 | Plasma HIV-1 RNA levels and genotype in participants living with HIV (GS-US-200-4072)

GS-6207 Dose	Participant ID	Baseline (day 0) HIV-1 RNA (log_{10} copies ml^{-1})	Maximum HIV-1 RNA change through day 9 (log_{10} copies ml^{-1})	Capsid genotype (day 9) (relative to baseline sequence)
20 mg	20-1	4.84	-0.83	wild-type
	20-2	3.86	-1.58	wild-type
	20-3	4.90	-1.74	Q67Q/H
	20-4	4.19	-1.43	wild-type
	20-5	4.21	-1.33	wild-type
	20-6	4.73	-1.21	ND
50 mg	50-1	4.01	-2.39	ND
	50-2	4.81	-1.55	wild-type
	50-3	4.3	-1.61	wild-type
	50-4	4.33	-2.32	ND
	50-5	4.85	-1.16	wild-type
	50-6	4.32	-1.73	ND
150 mg	150-1	4.61	-2.06	ND
	150-2	4.55	-1.68	wild-type
	150-3	4.58	-1.86	wild-type
	150-4	4.25	-1.49	ND
	150-5	4.61	-1.87	wild-type
	150-6	4.31	-1.62	ND
450 mg	450-1	4.31	-2.32	ND
	450-2	4.38	-2.86	ND
	450-3	4.53	-2.11	ND
	450-4	4.84	-1.83	wild-type
	450-5	4.44	-1.58	wild-type
	450-6	4.62	-2.52	ND

ND, not determined owing to repeated sequence assay failures.

nature research

Corresponding author(s): Stephen Yant

Last updated by author(s): Mar 11, 2020

Reporting Summary

Nature Research wishes to improve the reproducibility of the work that we publish. This form provides structure for consistency and transparency in reporting. For further information on Nature Research policies, see Authors & Referees and the Editorial Policy Checklist.

Statistics

For all statistical analyses, confirm that the following items are present in the figure legend, table legend, main text, or Methods section.

n/a	Confirmed
☐	☒ The exact sample size (*n*) for each experimental group/condition, given as a discrete number and unit of measurement
☐	☒ A statement on whether measurements were taken from distinct samples or whether the same sample was measured repeatedly
☐	☒ The statistical test(s) used AND whether they are one- or two-sided *Only common tests should be described solely by name; describe more complex techniques in the Methods section.*
☒	☐ A description of all covariates tested
☒	☐ A description of any assumptions or corrections, such as tests of normality and adjustment for multiple comparisons
☐	☒ A full description of the statistical parameters including central tendency (e.g. means) or other basic estimates (e.g. regression coefficient) AND variation (e.g. standard deviation) or associated estimates of uncertainty (e.g. confidence intervals)
☒	☐ For null hypothesis testing, the test statistic (e.g. *F*, *t*, *r*) with confidence intervals, effect sizes, degrees of freedom and *P* value noted *Give P values as exact values whenever suitable.*
☒	☐ For Bayesian analysis, information on the choice of priors and Markov chain Monte Carlo settings
☒	☐ For hierarchical and complex designs, identification of the appropriate level for tests and full reporting of outcomes
☒	☐ Estimates of effect sizes (e.g. Cohen's *d*, Pearson's *r*), indicating how they were calculated

Our web collection on statistics for biologists contains articles on many of the points above.

Software and code

Policy information about availability of computer code

Data collection

EnVision Manager 1.13.3009 was used to collect luminescence data.
JEOL JEM-1230 transmission electron microscope was used to collect images of ultra-thin sectioned HIV-1 virions.
SoftMax Pro 6.3.1 was used to collect CA in vitro assembly and p24 ELISA data.
ImageJ 1.46 was used to collect and quantify western blot data.
VnmrJ (versions 3.2A and 4.2A) and Topspin 4.0.6 and 3.5pl7 softwares were used to acquire NMR data.
Thermo Scientific Xcalibur 2.0.0.0 was used to collect LC/MS data.
X-ray crystallographic coordinates were collected on beamline 5.0.1 at Advanced Light Source, Berkeley, CA.
Quantstudio Real-Time PCR v1.3 was used to acquire quantitative RT-PCR data
BioRad Quantasoft Version 1.6.6.0320 was used to collect droplet digital PCR data.
Thermo Scientific Xcalibur 4.1.50 was used to collect high-resolution mass spectrometry data.

Data analysis

GraphPad Prism 7.0 was used to represent data and for statistical analyses.
SoftMax Pro 6.3.1 was used to analyze CA in vitro assembly and p24 ELISA data.
ProteOn Manager 3.1.0 or Scrubber 2.0 was used to analyze surface plasmon resonance biosensor binding data.
ImageJ 1.46 was used for quantification of western blots.
Sequencher 4.9 was used for DNA sequence analyses.
PyMOL 2.3.0 was used to analyze protein/small-molecule X-ray co-crystallography structures.
MacSynergy II version 1.0 was used to analyze synergy/antagonism of in vitro drug combinations.
Phoenix WinNonlin 6.4 was used for noncompartmental analyses of pharmacokinetic (PK) parameters.
MestReNova 11.0.4-18998 was used to analyze NMR data.
Waters Empower 3 version FR3 was used to analyze HPLC data.
Thermo Scientific Xcalibur 2.0.0.0 and 4.1.50 was used to analyze LC/MS and high-resolution mass spectrometry data, respectively.

For manuscripts utilizing custom algorithms or software that are central to the research but not yet described in published literature, software must be made available to editors/reviewers. We strongly encourage code deposition in a community repository (e.g. GitHub). See the Nature Research guidelines for submitting code & software for further information.

Data

Policy information about availability of data

All manuscripts must include a data availability statement. This statement should provide the following information, where applicable:

- Accession codes, unique identifiers, or web links for publicly available datasets
- A list of figures that have associated raw data
- A description of any restrictions on data availability

All data to understand and assess the conclusions of this research are available in the main text and Supplementary Information. Raw gel source data for Fig. 2f is available in Supplementary Figure 1. Small molecule X-ray crystallographic coordinates and structure factor files have been deposited in the Protein Data Bank (PDB, www.rcsb.org) with accession number 6V2F. Study GS-US-200-4072 was registered with ClinicalTrials.gov, NCT03739866. The datasets generated during and/or analyzed during the current study are available from the corresponding author on reasonable request.

Field-specific reporting

Please select the one below that is the best fit for your research. If you are not sure, read the appropriate sections before making your selection.

☒ Life sciences ☐ Behavioural & social sciences ☐ Ecological, evolutionary & environmental sciences

For a reference copy of the document with all sections, see nature.com/documents/nr-reporting-summary-flat.pdf

Life sciences study design

All studies must disclose on these points even when the disclosure is negative.

Sample size	No samples size calculation was performed. Sample sizes were chosen to provide a minimum of two independent samples in each of a minimum of 3 independent experiments in order to generate a convincing and reproducible result. If after doing so, the data did not produce convincing and reliable results with reasonably low standard deviations, additional experiments were performed to better assess the reproducibility of the phenotype under investigation. Exceptions were the virus-based electron microscopy experiment, which was performed twice. To ensure a reliable result in this instance, we analyzed >500 virions across multiple independent image fields at two different magnifications to rigorously assess the effect of each treatment on HIV-1 virion morphology. Results from those studies were quantified in a blinded fashion over 16 representative images to evaluate their statistical significance and to ensure the data presented were truly representative. The time-of-addition studies involved two independent experiments, each using 8 replicate cell cultures for each condition and time point, and produced similar results. The quantitative PCR studies used triplicate cell cultures for each of 3 time points in each of two independent experiments and produced similar results. The determination of peak replication level for wild-type and CA mutant HIV-1 variants involved two independent experiments, each using 6 replicate cell cultures originating from a mixture of CD4+ T cells isolated from 4 independent PBMC donors, and produced similar results. The dose-escalation drug resistance selection with GS-6207 was performed once using two replicate cell cultures and produced similar results. No sample size calculation was performed for clinical Study GS-US-200-4070. The sample size in this study is determined based on practical considerations and past experience with similar types of studies. A sample size of 40 subjects across 4 cohorts (10 subjects per cohort, including 8 active and 2 placebo) will provide a suitable assessment of the descriptive PK and safety profile. For clinical Study GS-US-200-4072, a sample size of 6 subjects in each of 4 GS-6207 dose groups and a total of 8 subjects in the placebo group will provide 99% power to detect a treatment difference of 2.79 log10 copies/mL in maximum reduction of HIV-1 RNA between at least one of the GS-6207 dose groups and the placebo group. In this power analysis, it is assumed that a common standard deviation for maximum reduction in HIV-1 RNA is 0.526 log10 copies/mL (based on Study GS-US-141-1219) and a 2-sided t-test is conducted at an alpha level of 0.05.
Data exclusions	No data sets were excluded.
Replication	The majority of in vitro experiments were repeated at least three times to ensure reproducibility. All attempts at replication were successful. For clinical trial studies, the analyses were performed on individual trial participants. Experiments did not include replicates as all participants and data points are unique.
Randomization	Not relevant to any of the in vitro studies as samples and corresponding controls were always processed at the same time. For each group in clinical studies GS-US-200-4070 and GS-US-200-4072, trial participants were randomized in a 4:1 and 3:1 ratio within each cohort, respectively, to receive either the drug (GS-6207) or placebo (vehicle alone).
Blinding	No blinding was done for any of the in vitro studies, except for each of the two studies evaluating the effect of drug treatment on capsid morphology. In both of these instances, virus-based electron microscopy images were collected in a blinded fashion by one individual at an external organization (Gladstone Institute) and then the associated virion phenotypes within each image (normal, abnormal, and immature) were scored and quantified in a blinded fashion by a research colleague. All other in vitro studies were conducted in an unblinded manner and instead were repeated multiple times each with multiple independent biological replicates to ensure reproducibility and, if appropriate, evaluate statistical significance of any observed phenotypes. Both clinical studies were double-blinded and placebo-controlled.

Reporting for specific materials, systems and methods

We require information from authors about some types of materials, experimental systems and methods used in many studies. Here, indicate whether each material, system or method listed is relevant to your study. If you are not sure if a list item applies to your research, read the appropriate section before selecting a response.

Materials & experimental systems

n/a	Involved in the study
☐	☒ Antibodies
☐	☒ Eukaryotic cell lines
☒	☐ Palaeontology
☒	☐ Animals and other organisms
☐	☒ Human research participants
☐	☒ Clinical data

Methods

n/a	Involved in the study
☒	☐ ChIP-seq
☒	☐ Flow cytometry
☒	☐ MRI-based neuroimaging

Antibodies

Antibodies used

Anti-HIV-1-p24 mouse monoclonal antibody (Thermo Fisher Scientific, Cat # MA1-71516, clone N17_05-004, Lot # SH2424811, 1:1000 dilution) was used for Western blot analysis.
Anti-alpha-tubulin rabbit monoclonal antibody (Cell Signaling Technology, Cat # 2125S, clone 11H10, lot # 11, 1:2000 dilution) was used for Western blot analysis.
HRP-conjugated goat anti-rabbit polyclonal antibody (Thermo Fisher Scientific, Cat # 31460, lot # SA245916, 1:5000 dilution) was used for Western blot analysis.
HRP-conjugated goat anti-mouse polyclonal antibody (Thermo Fisher Scientific, Cat # 31430, lot # RK244131, 1:5000 dilution) was used for Western blot analysis.

Validation

All antibodies were validated by manufacturers and in previous publications.

HIV1 p24 Monoclonal Antibody (N17 (05-004)) from Thermo Fisher Scientific is a mouse monoclonal antibody generated using recombinant p24 protein of HIV-1 B-subtype consensus purified from E. coli as the immunogen. It reacts with HIV-1 and has been shown to work in applications such as ELISA (1:10,000) and Western Blot (1:1,000). This antibody reacts with HIV-1 p24 subtypes B, C and A, and has been mapped to the C-terminus, aa 165- 231, which are well outside all of the N-terminal capsid mutations assessed in this new report. The manufacturer shows that this antibody detects recombinant HIV-1 Gag (Han-2 subtype) by Western blot analysis. Our data presented here also confirm this antibody does not cross-react with host cell proteins in mock-transfected samples.

α-Tubulin (11H10) Rabbit mAb #2125 from Cell Signaling Technology is a rabbit monoclonal antibody generated using a synthetic peptide corresponding to the amino terminus of human α-tubulin protein as the immunogen. It has been validated for Western blot applications (1:1,000 dilution) and the manufacturer shows that it detects endogenous levels of total α-tubulin protein and does not cross-react with recombinant β-tubulin. It shows reactivity with Human, Mouse, Rat, Monkey, D. melanogaster, Zebrafish, Bovine, and Pig and is predicted to react with Dog based on 100% sequence homology. There are currently 17 citations using this antibody for Western blot analysis again human α-Tubulin.

Eukaryotic cell lines

Policy information about cell lines

Cell line source(s)

MT-2 and MT-4 cell lines were obtained from the NIH AIDS Reagent Program.
HEK293T cells were obtained from the Gladstone Institute for Virology and Immunology. Huh-7 cells were obtained from ReBLikon GmbH. HepG2, PC-3, and MRC-5 cell lines were obtained from the American Type Culture Collection.

Authentication

No authentication.

Mycoplasma contamination

All cell lines were tested and judged free of mycoplasma contamination using a commercial kit.

Commonly misidentified lines
(See ICLAC register)

None of the cell lines used are commonly misidentified cell lines.

Human research participants

Policy information about studies involving human research participants

Population characteristics

Leucopacks were purchased from AllCells (Alameda, CA, USA). Donors underwent a screening process at three month intervals and attributes, such as age, sex, HLA typing, and medical history, were captured during each screening. Screening is done for viral status, CBC, changes in health status (illness, medication use). Donors utilized herein included both genders, ranged in age from 18 - 50, and most importantly for the sake of the studies described herein, all were negative for HIV-1, hepatitis B virus, and hepatitis C virus infections. All donors were obtained from the Alameda California location and were deemed medication-free

(i.e., no over the counter, prescription, birth control, steroid drugs, or vitamins/supplements used for the 2 days prior to sample collection) to avoid any confounding effects due to unforeseen drug-drug interactions.

For clinical Study GS-US-200-4070, we enrolled HIV-1-uninfected healthy men and women, 18-45 years of age.
For clinical Study GS-US-200-4072 (registered with ClinicalTrials.gov, NCT03739866), we enrolled treatment-naive or -experienced, but HIV capsid inhibitor naïve and integrase strand transfer inhibitor naïve, men or nonpregnant, nonlactating women, 18–65 years of age with plasma HIV-1 RNA levels ≥ 10,000 copies/ml but ≤ 400,000 copies/ml and CD4+ T cell counts > 200 cells/mm3.

Recruitment

For clinical Study GS-US-200-4070, eligible HIV-1-uninfected healthy men and nonpregnant, nonlacting women, 18-45 years of age, negative for HIV-1 and HCV antibodies and HBV surface antigen, were enrolled in the study sequentially. As this study enrolled from a single site (Quotient Sciences - Miami LLC) in Florida, the study participants were mostly young and healthy people who were willing to participate in clinical trials from the Miami metropolitan area. For example, the study participants were mostly Hispanic or Latino males in their 30s.

For clinical Study GS-US-200-4072, eligible viremic participants were pre-screened for sensitivity to BIC/FTC/TAF. Participants harboring sensitive viruses were enrolled in the study sequentially. As this study enrolled mostly treatment naive people, the study population reflected the current HIV epidemic in the US. For example, the study participants were mostly non-Hispanic (or Latino) White or Black males in their 30's.

We acknowledge there is a potential for bias for both studies. However, we believe that the data generated from both studies are valid and sufficient to support further clinical development of GS-6207, where we will evaluate GS-6207 in a larger and more diverse population.

Ethics oversight

The leukopack collection protocols and donor informed consent were approved by an Institutional Review Board (IRB) at AllCells, with strict oversight. HIPAA compliance and approved protocols are also followed. Donors are screened and tissues are collected in accordance with GMP, FDA, CFR 21CFR1271 and EU directives 2004/23/EC and 2006/17/EC.

The clinical trials were conducted in accordance with Good Clinical Practice, as defined by the International Conference on Harmonisation and in accordance with the ethical principles underlying the United States Code of Federal Regulations, Title 21, Part 50 (21CFR50). The protocol and the subject informed consent form received institutional review board/independent ethics committee approval/favorable opinion (Advarra, Columbia, MD) before initiation of the study. Freely given written informed consent was obtained from every subject before participation in the clinical studies.

Note that full information on the approval of the study protocol must also be provided in the manuscript.

Clinical data

Policy information about clinical studies

All manuscripts should comply with the ICMJE guidelines for publication of clinical research and a completed CONSORT checklist must be included with all submissions.

Clinical trial registration

NCT03739866 (GS-US-200-4072).
GS-US-200-4070 is not registered with ClinicalTrials.gov, as it is a Phase 1 study, where the primary goal is to determine the antiviral activity and pharmacokinetics of GS-6207.

Study protocol

The full protocol for Study GS-US-200-4072 is not publicly available, because it is not a Phase 2 or 3 studies, but a Phase 1 study, where the primary goal is to determine the antiviral activity and pharmacokinetics of GS-6207. As Phase 1 studies, CONSORT checklist is not needed per Nature Research policy information about clinical studies.

Data collection

Participants for Study GS-US-200-4070 were enrolled from a single site in the United States: Quotient Sciences (Miami, FL), which specializes in Phase 1 studies in healthy volunteers. First participant was enrolled on 16 February 2018, and the last one on 12 July 2018. Last participant last observation was on 21 February 2019. Database finalization occurred on 24 May 2019, and treatment unblinding on 06 June 2019.

Participants for Study GS-US-200-4072 were enrolled across 5 clinical sites within the United States, which are clinics where people living with HIV are diagnosed, treated, and followed: the Ruane Clinical Research Group, Inc. (Los Angeles, CA), the Lundquist Institute for BioMedical Innovation at Harbor-UCLA Medical Center (Torrance, CA), AIDS Arms, Inc., DBA Prism Health North Texas (Dallas, TX), North Texas Infectious Diseases Consultants (Dallas, TX), Tarrant County Infectious Disease Associates (Fort Worth, TX), and the Crofoot Research Center, Inc. (Houston, TX). The first participant for the 20-450 mg cohorts was enrolled on 08 January 2019, and the last one on 09 July 2019. The last participant, last observation for these cohorts is projected to be on 18 February 2020. Database finalization is projected to occur on 21 August 2020. This study is still blinded and ongoing.

Outcomes

For Study GS-US-200-4070, the primary and secondary outcome measures were pre-defined as per the usual first-in-human study in healthy volunteers. The outcome measures were assessed using conventional methods as follows:
-Primary outcome measures: safety and pharmacokinetics (AUCinf, AUClast, %AUCexp, Cmax, Tmax, Clast, Tlast, lambda z, CL/F, t1/2, and Vz/F).
-Secondary outcome measures: none

For Study GS-US-200-4072, the primary and secondary outcome measures were pre-defined as per the usual proof-of-concept study in people living with HIV. The outcome measures were assessed using conventional methods as follows.
-Primary outcome measures: maximum reduction of plasma HIV-1 RNA (log10 copies/mL) from Day 1 through Day 10
-Secondary outcome measures: safety and pharmacokinetics (AUC0-t, AUCinf, AUClast, CL/F, t1/2, lambda z, Vz/F, Cmax, Tmax, Clast, CD10, Tlast)